

We are IntechOpen, the world's leading publisher of Open Access books Built by scientists, for scientists

6,900

Open access books available

186,000

International authors and editors

200M

Downloads

Our authors are among the

154

Countries delivered to

TOP 1%

most cited scientists

12.2%

Contributors from top 500 universities



WEB OF SCIENCE™

Selection of our books indexed in the Book Citation Index
in Web of Science™ Core Collection (BKCI)

Interested in publishing with us?
Contact book.department@intechopen.com

Numbers displayed above are based on latest data collected.
For more information visit www.intechopen.com



EMC Analysis of Railway Power Substation Modeling and Measurements Aspects

S. Baranowski¹, H. Ouaddi¹, L. Kone¹ and N. Idir²

¹*Université Lille 1 Sciences et Technologies, USTL, IEMN/TELICE Laboratory*

²*Université Lille 1 Sciences et Technologies, USTL, L2EP Laboratory,
F-59650 Villeneuve d'Ascq,
France*

1. Introduction

The first part of the chapter will present the global aspect of the railway power infrastructures and specially the power supply substation. The goals of this study consist in proposing a high frequency model of the railway systems and verifying by simulation the conformity with the EMC standards. Thus, each component of the railway power infrastructure (transformer, power rectifier) is modeled and the simulation results of the conducted emissions are compared to measurements on a reduced scale of the power supply substation.

2. EMI sources in railway system

A railway system might pollute, in an electromagnetic sense, the surrounding environment, disturbing radio and communication systems which can be not related to the railway itself. In this case the whole railway can be considered as a source of Electromagnetic Interference (EMI). In order to avoid the disruption of the electronic equipments near to the railway, the overall field generated by railway system must be kept below certain safety values given by standards [1]. Obviously, there are many sources of the electromagnetic field and their contributions can come from:

- Each part of the railway: for example, a locomotive or the power supply substation can induce EMI that exceed the EMC standards limits set for the electromagnetic field, because of power circuits that might become a source of emissions.
- The whole system: the power supply line (cable) can behave as an antenna, which radiates an electromagnetic field proportional to the current. The spectrum and the intensity of the current depend not only on the power absorbed by a train, but also from the structure (geometrical dimensions ...) of the line, that may cause resonances as shown in Fig.2.

However, a train might be or be not compliant to field standards depending on the line characteristics and on its position on the railway. Nowadays, trains are designed to meet EMC rules, but the non-compliances can be remedied thanks to identification of the different resonances frequency, which can occur mainly in a frequency range from some kilohertz up to one gigahertz.

2.1 Description of standards EMI measurement methods

The EMC standard EN 50121 [1] is used to characterize the EM environment, in the railway systems; it notably aim to limit the EMI levels from the railway infrastructures to the external environment. This standard EN 50121 describes the methodologies and the limits to apply, relating to the EM radiations and immunity of railway equipments, vehicles and infrastructures. The emissions of the whole railway system, including vehicles and infrastructure, are dealt with the section 2 of the EN 50121. The objective of the tests specified in this standard is to verify that the EM emissions produced by the whole railway systems do not disturb the neighboring equipments and systems.

The methodology then consists in measuring the radiated EM emissions at a distance of 10 m from the middle of the tracks and at about 1.5 m from the floor (Fig.1) and in comparing them with the maximum levels (limit curve in red in Fig.2). The measurements protocol and the limits are specified for the frequencies varying from 9 kHz to 1 GHz.

For each frequency band (9kHz-150kHz; 150kHz-30MHz; 30MHz-1GHz), the standards define among others:

- which component of field, magnetic (up to 30MHz) or electric (above 30 MHz), has to be measured,
- the resolution bandwidth (RBW) of the spectrum analyzer that must be used for the measurements. Then the limit curve depends on these parameters and is not a constant as shown until 1MHz in fig.2

During measurements of the electromagnetic field radiated at 10 m from the railway track, we can observe that, sometimes, for some frequency, the standards limit can be exceeded. An example of measurement from 10 kHz to 1 MHz is given in fig. 2. The exceeding is characterized by resonance phenomena which appeared for some frequencies of the power supply current.

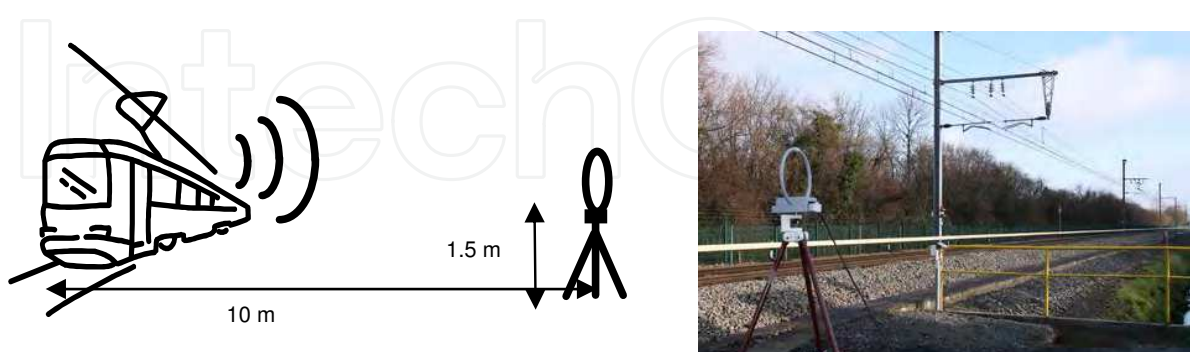


Fig. 1. On site measurement of the electromagnetic radiation of the train (stationary and moving)

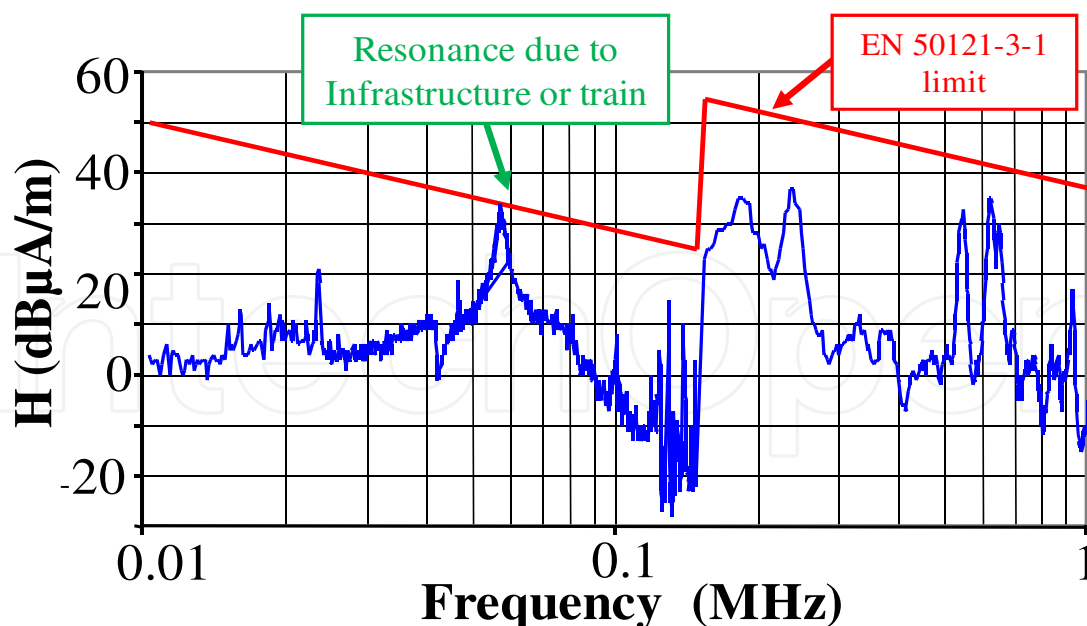


Fig. 2. Example of the measured magnetic field

2.2 Effect of the resonances

As presented previously, the aim of the standards is to limit the disturbance of the external environment produced by the railway infrastructure but also on the railways system itself. Indeed, the new generation of rolling stock is equipped with safety communication systems with on board antennas which must not be disturbed neither. These elements of safety system operate in frequency range from 10 kHz to 30MHz, which constitute the frequency range considered in this study but also above, for example, the GSMR signal frequency is around 900MHz. Thus, it becomes important to know which source can introduce the disturbances.

Besides, sensitivity of these communication systems must also be evaluated for the resonant frequencies.

3. Railway power infrastructures

A schematic representation of the railway infrastructure is shown in Fig. 3. In this figure, we can see that the power supply system constituted by the substation, the rails, the catenaries and the train which constitutes the load of the power line. This figure also shows a location system based on telecommunication between on board antenna and antenna along the track.

The railway power supply system is generally composed by two main systems:

- The first one is the “lines system” constituted by the catenaries and the rails; this transmission line has already been modeled in a previous work [2], taken into account all important parameters in an EMC point of view (non uniformity and camber of the lines, multi-conductors structures, conductivity of the ballast, ...)
- The second main part is defined by the power supply substation which contains often a power transformer, sometimes static converters, and cables, bus bars...etc.

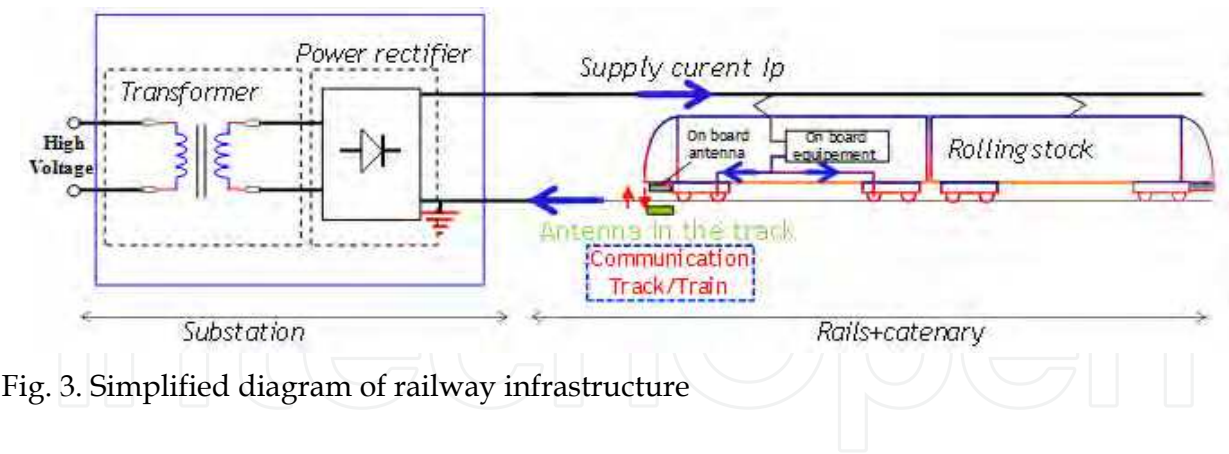


Fig. 3. Simplified diagram of railway infrastructure

4. Problem of EMC in railway

In order to avoid EMI with high levels of electromagnetic disturbances, measurements are usually performed. Test results can lead to different comments and from an industrial point of view, it is important to distinguish the disturbances due to the railway power supply infrastructure (substation – line catenaries/rail) and others due to the train itself. Indeed, it is important to know which kind mitigations solutions have to be done to reduce the disturbances and who should do that: the train manufacturer or the power supplier.

In a previous research project [2], the lines system has been modeled. The proposed model enables to estimate the field radiated by the power line taken into account various parameters like the geometry of the line; the conductivity of the soil ... The model is based on line theory, the train is the load (Z_{train}) and a generator feeds the lines.

An example of the simulation conditions and the obtained results is given in figures 4 and 5

This model gives good results and many details on how each parameter has been taken into account can be found in [2]. But it is only a model of the lines and the generator used in this simulation is a sinusoidal one with constant amplitude.

Then, it was necessary to model the power substation to obtain a more realistic generator and this has constituted the goal of the CEMRAIL project of which some results are presented here.

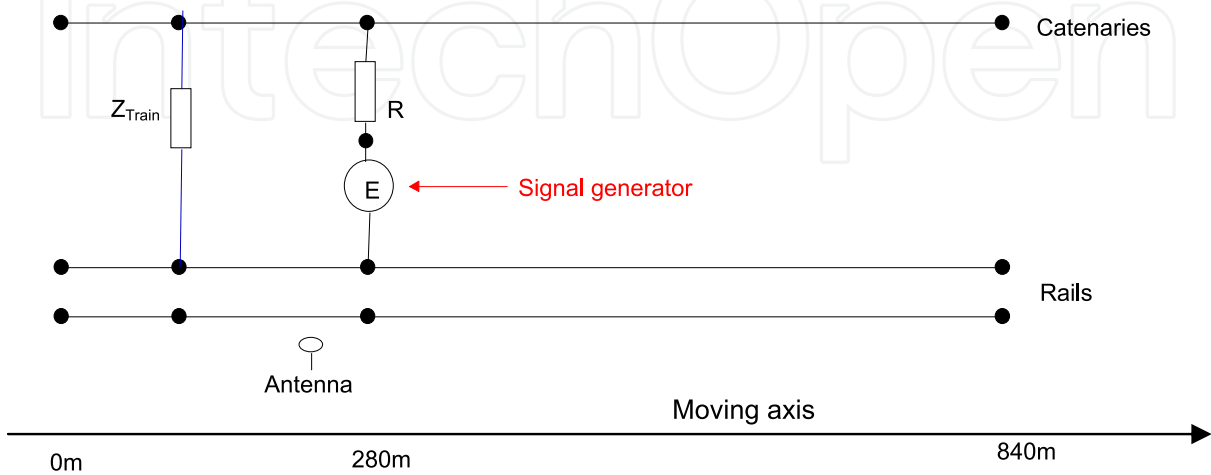


Fig. 4. Simplified model of the power supplier line

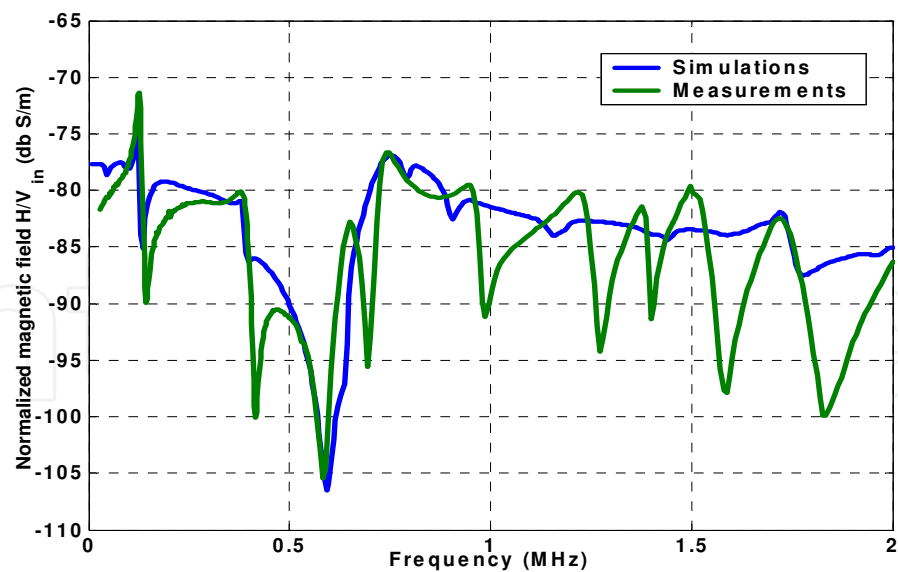


Fig. 5. Example of obtained results (corresponding to the Fig. 4 configuration). The generator give a sinusoidal signal of 1V amplitude.

5. Power supply substation

In the world, many kind of railway power supply exist: alternative (AC) or direct current (DC), with various amplitudes: 1500kV, 3kV, 25kV... Then, we have worked on a general power substation constituted by a transformer and a power converter as presented in fig. 6.

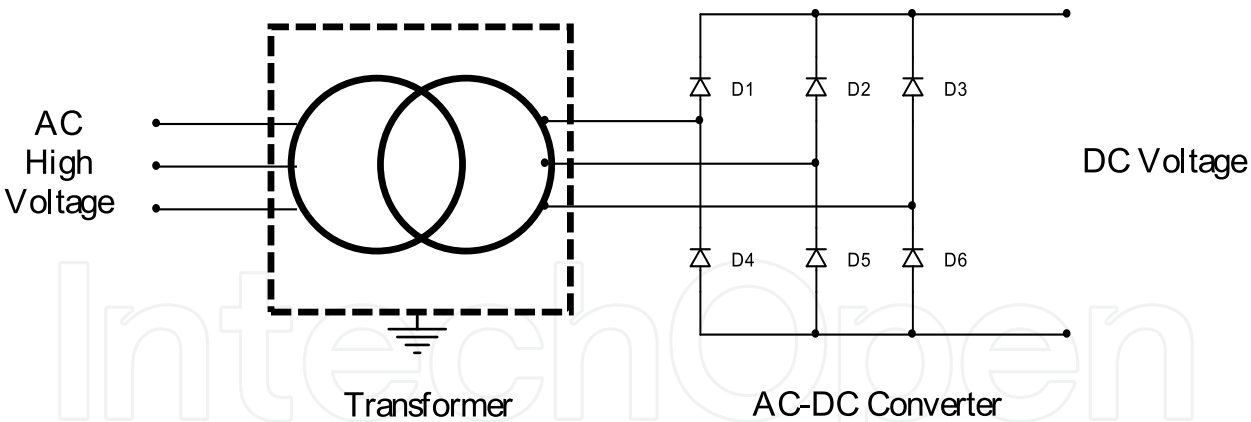


Fig. 6. Schematic circuit of a railway substation

In case of AC power supply substation, there is no AC/DC converter. The power transformer constitutes the main device of the substation.

In order to propose a high frequency model of the whole system, it's necessary to determine a model for each element, especially of power transformer, which accuracy will be highly dependent of the accuracy of each primary model. The low frequency model of the transformer, defined at 50Hz, is not valuable when the frequency increases. Indeed, some phenomena can be predominant in high frequencies as the Eddy current, which depends on the variation of the magnetizing impedance and the winding resistance, but also the

parasitic capacitances which appear between windings due to the insulated parts of the transformer. The analysis of the transformer behavior shows that it's possible to use an equivalent electrical circuit model which is valid in the considered frequency band.

During the past decades, many models of power transformer have been studied for several applications. Most of those models, often in a reduced frequency band, are based on the representation of the transformer by an arrangement of resistive, inductive and capacitive elements which can take into account the physical behavior of power transformer [3]; some others are wide band models established using the black box principle [7]. Obviously, it's also possible to apply the FEM (Finite Element Method) method to have a precise model, but in this case, the exact constitution of the transformer must be known. Some additional difficulties are found in the studied problem: how to found the appropriate data sheet when the transformer is operated in the railway system since many years? In the following sections, we will present the proposed equivalent model and two techniques used to identify the transformer parameters.

6. High frequency model of transformer

6.1 Preliminary study

Making measurements in railways power substation is not easy, then preliminary investigations have been done on various power transformers. Primary and secondary winding impedances measurements in various configurations have been done on two different transformers:

- 15 kVA three phase laboratory transformer,
- 2.38 MVA train power transformer.

Figure 7-a (15kVA transformer) and Fig. 7-b (2.38MVA transformer) show the secondary winding impedance measured when the primary is short circuited for these two transformers.

These two impedances have been measured in the same frequency band: 100 kHz to 40MHz. We can note that these two responses are globally identical. Thus, we will model, in the first time, a low power transformer before to apply this model to a real substation transformer.

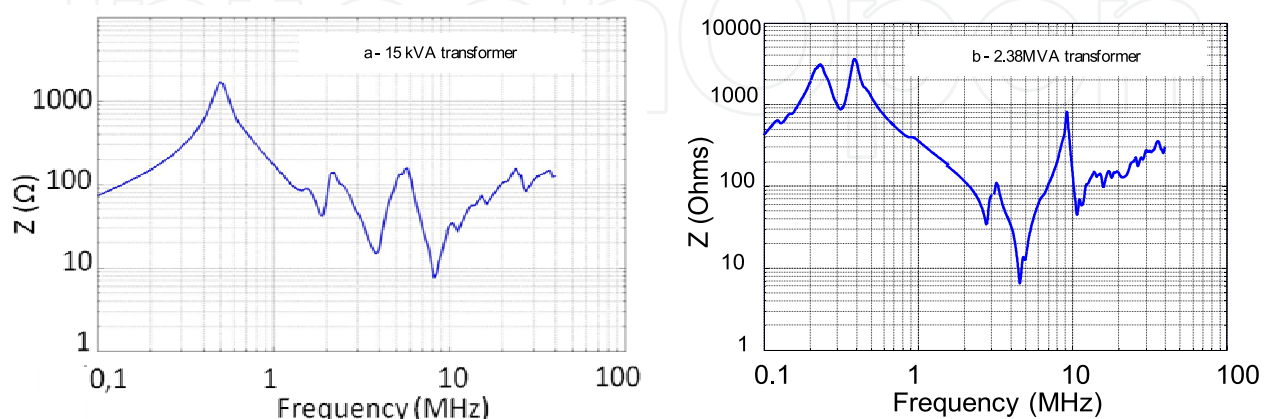


Fig. 7. Secondary winding impedance measurements when the primary is short circuited for two tested transformers (a- 15kVA and b- 2.38MVA)

6.2 Laboratory test bench

In order to analyze the behavior or the railway substation we have built a test bench which reproduces the substation in small scale.

The experimental setup is composed with a three phase power transformer, a diodes rectifier and loads. The transformer is a 15 kVA - 220 V/110 V with Δ connected high voltage (HV) winding and Δ connected low voltage (LV) winding. The power rectifier is designed with twelve power diodes and is connected to 47 Ω resistor. All these elements are placed over a common ground plane (Fig. 8). The different devices are connected using 1m long cable.

6.3 Transformer model

A high frequency model of the power transformer, which takes into account the various physical phenomena has been studied [4][8]. Figure 9 presents this model applied to the 15kVA three phase power transformer used in the laboratory test bench (fig.8).

Starting from an ideal transformer model with transformation ratio η , the proposed model takes into account, for each phase, the leakage inductances, the skin effects, the magnetizing impedance and stray capacitances of which become significant at high frequency. Moreover the iron core has been considered linear at frequency above 10 kHz [12] [13] consequently its effect can be neglected at high frequencies.

This model is valid in the frequency band varying from 40 Hz to 30 MHz.

The subject of the work is to identify the important physical parameters which contribute to induce resonance phenomena. We have chosen to propose a model as physical as possible and after, if necessary, to add black box to model more intricate phenomena.

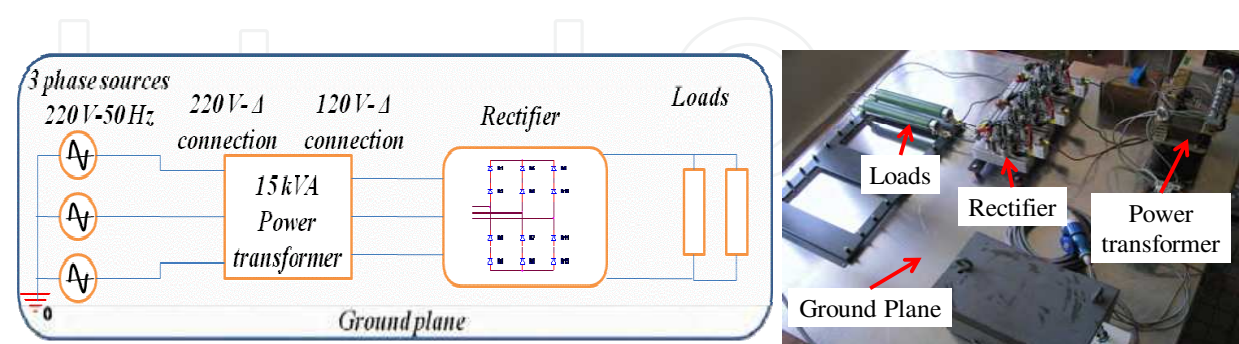


Fig. 8. Circuit diagram and photo of the test bench

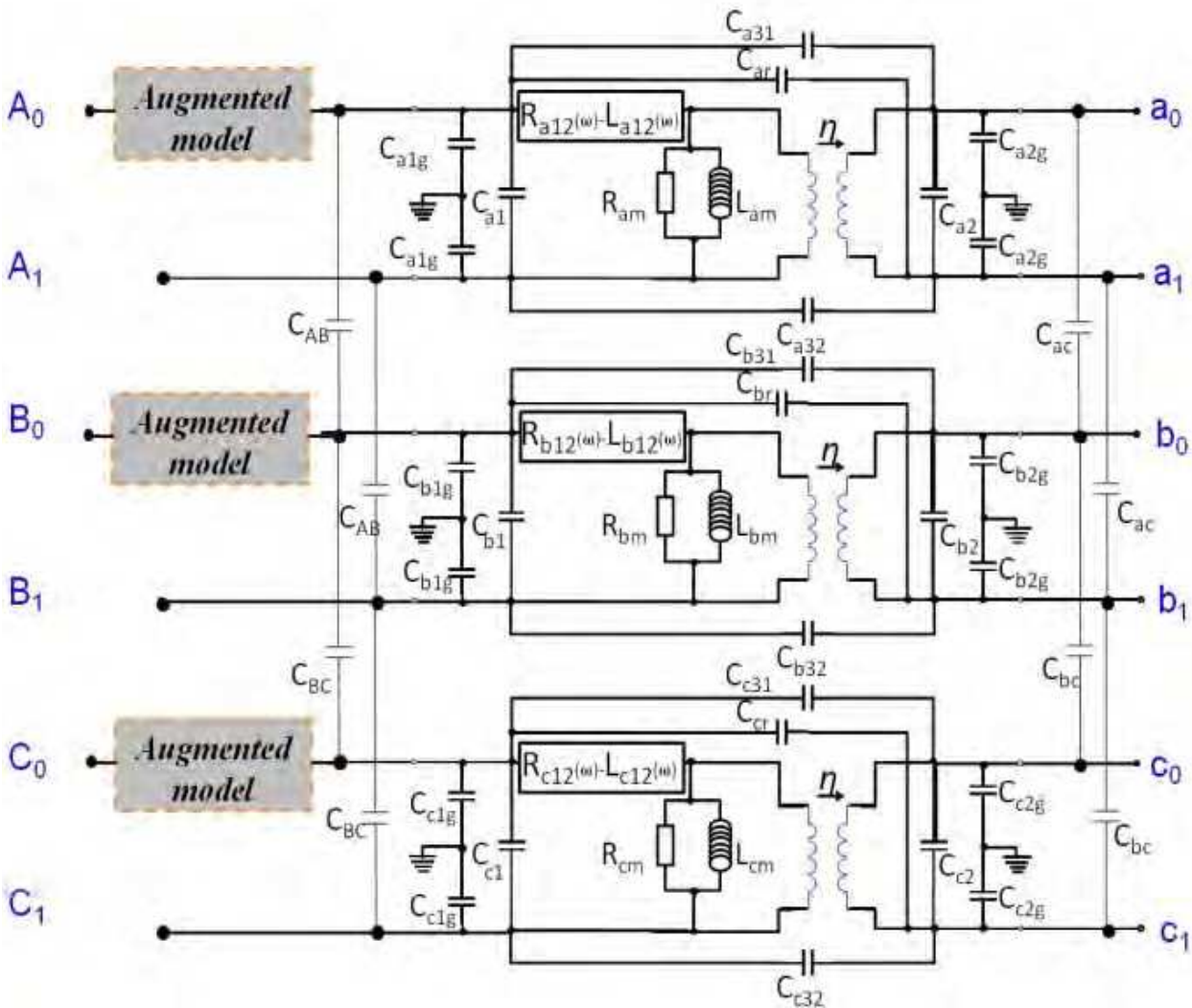


Fig. 9. High frequency model of three-phase power transformer

Each element of the equivalent circuit will be detailed and the method used to determine these parameters will be presented in the next section.

- The block $R_{a12} - L_{a12}$ ($R_{b12} - L_{b12}$ and $R_{c12} - L_{c12}$ resp.) shown in the Fig. 9 represents the leakage inductance and wire resistance (due to the skin effects) of the phase A (B and C resp.) [14].
- The magnetizing impedance is modeled thanks to a resistance (R_{am}) with an inductance in parallel (L_{am}) for phase A (resp. R_{bm} , L_{bm} and R_{cm} , L_{cm} for phase B and C resp.). Of course, the magnetizing impedance changes with the frequency [7] [15].
- In the proposed model, the considered capacitances, presented in fig 9, are listed below [16], [17] :
 - Turn-to-turn capacitance of the primary and secondary windings: $C_{a1}, C_{a2}, C_{b1}, C_{b2}, C_{c1}, C_{c2}$,
 - Capacitances between windings (divided in two capacitances): $C_{a31}, C_{a32}, C_{b31}, C_{b32}, C_{c31}, C_{c32}$,
 - Capacitance between the input of the primary winding and the output of the secondary: C_{ar}, C_{br}, C_{cr} ,

- Capacitances between the winding and the ground: $C_{a1g}, C_{a2g}, C_{b1g}, C_{b2g}, C_{c1g}, C_{c2g}$,
- Capacitances between the phases ($C_{AB}, C_{BC}, C_{ab}, C_{bc}$).
- Impedance called “augmented model”: the impedance measurements show fast fluctuations above 10 MHz (Fig.10) and their modeling using electric circuits can be time consuming. However, the use of macro model can be a good solution to take into account these fast variations at high frequency. These impedances are modeled by blocks named “augmented model” as shown in Fig.9 and defined by using vector fitting method; details are given in [4-5-6].

Note: The proposed model can be used to model a single phase transformer by using only one circuit by phase.

6.4 Validation results

The experimental results, in time or in frequency domain presented in the next sections, allow determining the various parameters of the proposed model. Figure 10 shows an example of modeling results compared to experimental data.

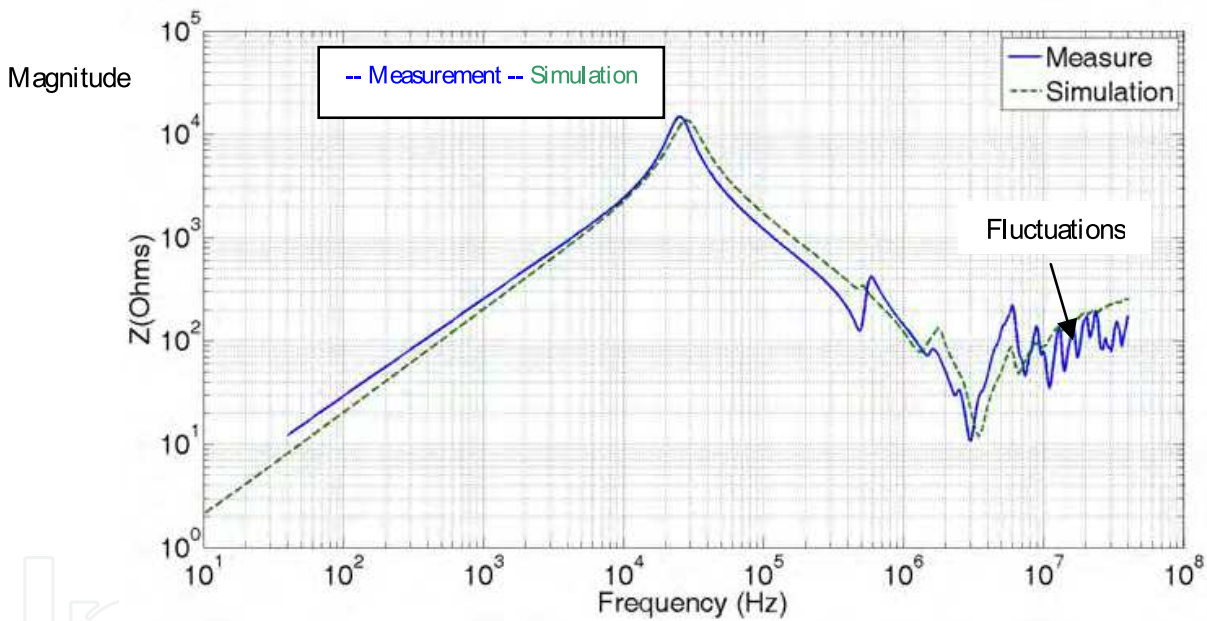


Fig. 10. Comparison within measurements and simulation results (impedance of the primary winding, the secondary being open)

7. Determination of the various elements of the transformer model

The determination of each parameter of the equivalent circuit (Fig.9) of the transformer model is realized from impedance measurements versus frequency, in different test configurations [7] [8].

7.1 The magnetizing impedance

The magnetizing impedance of each phase is modeled by a resistance in parallel with an inductance; their values are deduced from the impedance measured on the primary

winding, at low frequency, when the secondary winding is open as shown in Fig 11. The values of these parameters for the phase A and B are given as following:

$R_{am}= 13.44\text{ k}\Omega,$ and $L_{am}=31.19\text{ mH},$

$R_{bm}= 15.87\text{ k}\Omega$ and $L_{bm}=32.14\text{ mH}$

However, if we take into account the geometry of the transformer, phases A and C are considered, to have the same behavior, then the corresponding parameters are supposed to have the same value.

7.2 The leakage impedance

The leakage inductance and the wire resistance (the skin effect) of the winding can be determined by measuring the primary impedance when the secondary winding is short-circuited. Winding losses can be estimated from the impedance measured in the low frequency band as shown in Fig. 12.

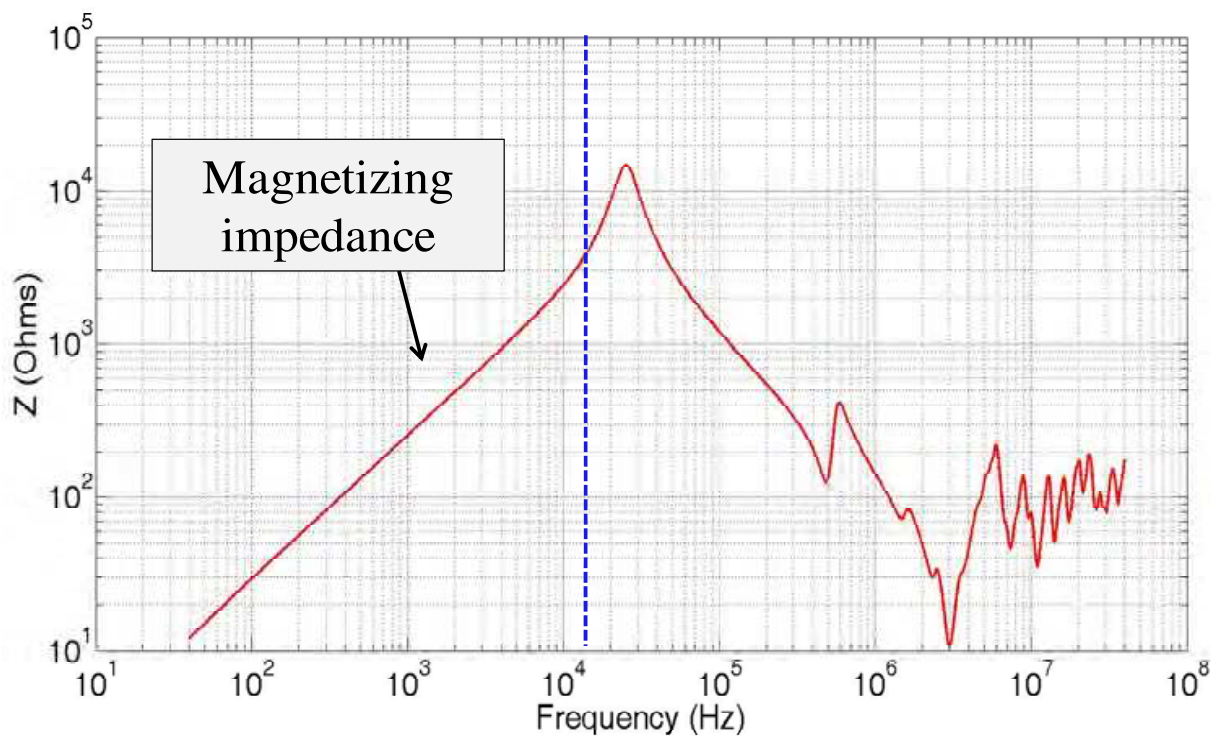


Fig. 11. Primary winding impedance when the secondary is opened (measuremens on the Phase A of the test bench transformer)

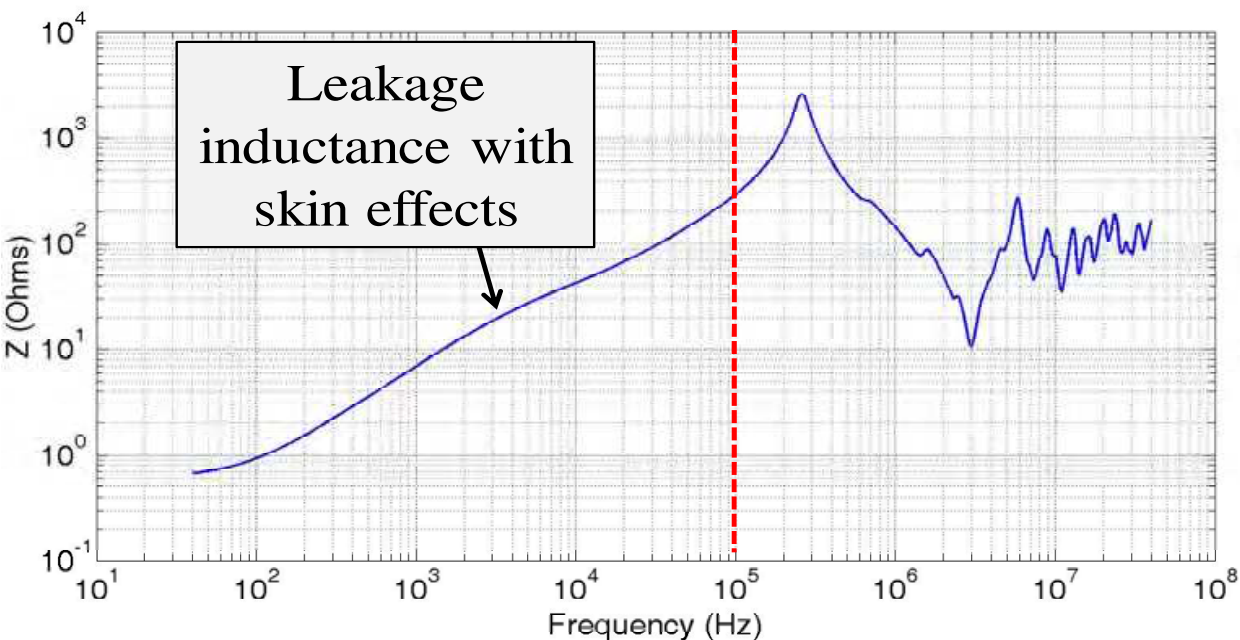


Fig. 12. Primary impedance with secondary short circuited (phase A)

The leakage impedance can be modeled using a R-L ladder network as shown in Fig. 13

In order to have an efficient approximation, the parameters of the equivalent circuit are computed with a less square algorithm; the identification being performed with the results of measurements.

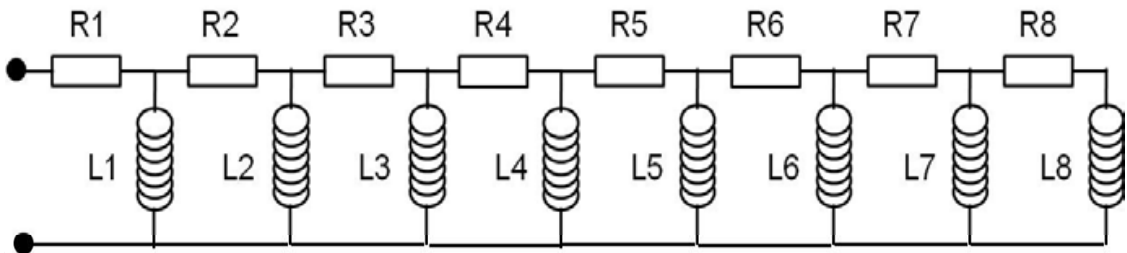


Fig. 13. Equivalent circuit of the leakage impedance

Table1 presents the parameters of the equivalent circuit of the leakage impedance obtained for the studied transformer.

R_i in Ω	R_1	R_2	R_3	R_4	R_5	R_6	R_7	R_8
Phase A	0.6	58	49	132	45	472	746	679
Phase B	0.6	58	0.001	33	37	1082	15	39
L_i in mH	L_1	L_2	L_3	L_4	L_5	L_6	L_7	L_8
Phase A	1.1	1.08	3.6	100	13	11	54	14
Phase B	1.1	2.3	2.4	2.5	8.3	11	36	69

Table 1. Parameters of the leakage impedance model of the laboratory transformer (phase C is supposed equivalent to phase A)

7.3 Stray Capacitances

The stray capacitances of each phase of the transformer are estimated separately. As an example, here, the phase A (A0A1-a0a1) is studied. The transformer is modeled as a “black box”, and it’s necessary to determine the capacitance Ca1, Ca2, Ca31, Ca32, Car, Ca1g and Ca2g. Their effects are located in high frequencies so they will be evaluated in this frequency range.

For each phase, seven measurement configurations are necessary to determine these capacitances. Thus, they provide seven equations which unknowns are the capacitances of the equivalent circuit. Following, the equation system is solved using mathematical tools. Figure 14 presents the seven measurements configurations with the associated equations, in the case of the phase A. The arrows show the measurements points, the short circuits are presented by the lines and Cme represents the measured capacitance. As well as the magnitude, the phase of the impedance is measured in order the make an efficient characterization.

Moreover some precautions are taken for example it is proper to short-circuit the two other phases when the third is characterized in order to inhibit their influences.

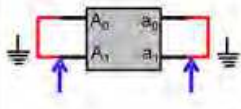
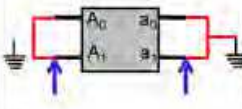
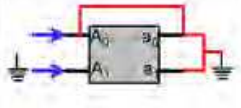
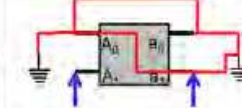
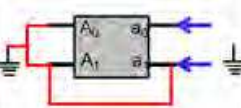
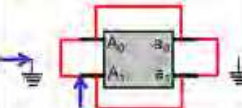

	$C_{me} = C_{ar} + C_{a32} + C_{a31} + \frac{2C_{a1g}C_{a2g}}{C_{a1g} + C_{a2g}}$		$C_{me} = C_{ar} + C_{a32} + C_{a31} + 2C_{a1g}$
	$C_{me} = C_{a1} + C_{a32} + \frac{C_{a1g}}{2}$		$C_{me} = C_{a32} + \frac{(C_{a1g} + C_{a1})}{C_{a1g} + C_{a1} + 1}$
	$C_{me} = C_{a2} + C_{a31} + \frac{C_{a2g}}{2}$		$C_{me} = 2C_{a2g} + 2C_{a1g}$
	$C_{me} = C_{a2} + C_{a32} + \frac{C_{a2g}}{2}$		

Fig. 14. Measurement configuration used for determining capacitances (example for phase A)

7.4 The augmented model impedance

The impedance characteristics presented in Figures 11 and 12 show the same evolution at high frequency (above 3 MHz) with fast variations and consequently it costs time to model. Thanks to "augmented method" [5], it is possible to consider this part by using an inductance in parallel with a "black box". The "black box" is elaborated by using the principle of the "vector fitting" [13]. This algorithm consists in approximating a frequency response with a rational function, expressed by a sum of partial fractions. This principle is implemented in the IdEM® software [6] [18] used for our study. This code generates a macro-model which could be integrated in software like Pspice. Figure 9 presents the main equivalent circuit of the transformer with the added impedance issued from "augmented model" (Fig.15) which takes into account the high frequency effects. Figure 16 shows the effect of this 'augmented model impedance' on the HF accuracy of the model, by comparison of the measurements results with the model ones.

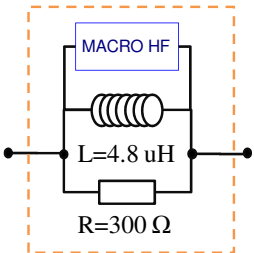


Fig. 15. Equivalent circuit for high frequency behavior of the transformer.

This circuit is represented by a component named "augmented model" in figure 9.

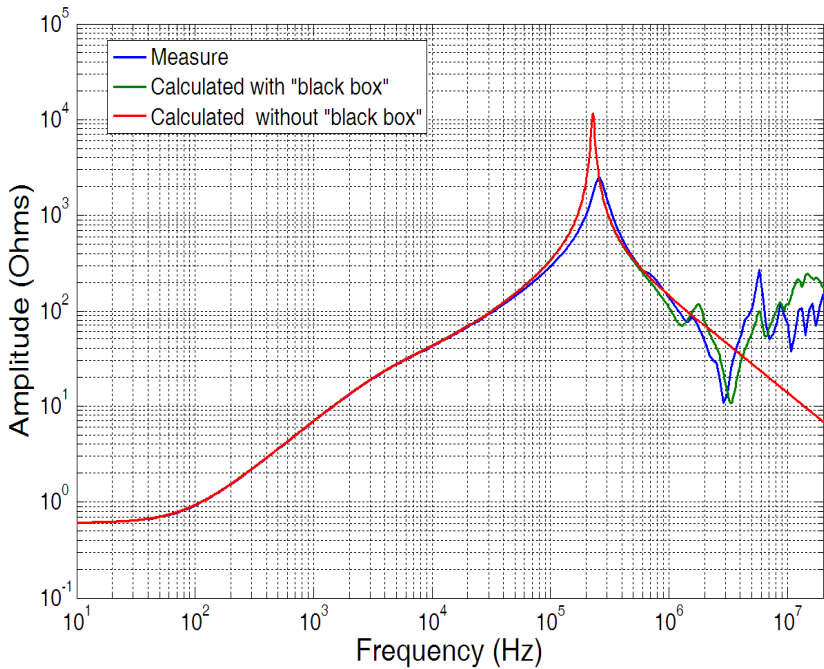


Fig. 16. Primary impedance with secondary short circuited (Phase A). Comparison between measurement and simulation result with and without the augmented model (named black box in the figure).

8. Characterization of the transformer in frequency domain

As detailed in the previous section, the determination of the proposed model parameters is based on impedance measurements which can easily be done in frequency domain with impedance or network analyzer.

This method gives good results for low power transformer but there are some problems to make this kind of measurement with very high power transformer as the ones used in railways substation, which are the followings:

- The connection between transformer and measurement apparatus (network or impedance analyzer) is not easy and some effects due to non ideal connection can be seen, especially at high frequency.
- The windings are often constituted with 'bus-bar' because the nominal power is high. Then, measurements with the previous apparatus are done with very low level signal compared to nominal power and can induce many errors (signal to noise ratio, non linearity effect).

We propose a measurement method, carried out in time domain and based on the injection of higher level signals in the transformer. The principle of the proposed method and the obtained results are presented in the next section. [9]

9. Characterisation in time domain

9.1 Measurements principle

A square voltage waveform is applied at terminals of the transformer in the various configuration tests. The input current and input voltage are measured in time domain and determined in frequency domain via Fourier transforms and then the corresponding impedance can be deduced.

This experimental method has been applied in reduced scale on the laboratory test bench, to characterize the 15kVA three phases transformer. For this characterization, a square signal of magnitude 30 V with a period equal to 30 μ s, duty cycle equal to 0.5 and the rise time and fall time equal to 10ns. A differential voltage probe (bandwidth: 100MHz) is used to measure the voltage at the generator terminals. The current is measured with a current probe (bandwidth: 100MHz). The connection wires between the generator and the transformer are chosen as short as possible. Figure 17 shows a diagram of the measurement bench; we can see the generator, one phase of the transformer and the position of measurements probes.

Figure 18 and 19 show respectively the waveforms of the primary voltage and current of one phase of the transformer, in the configuration described in figure 17 when the voltage signal is applied at the primary winding with the secondary being open. These measurements allow determining the magnetizing impedance. The sample frequency used for these measurements is 125 Msample/s. All impedances can then be measured with this technique, but now the data have to be processed.

9.2 Impedance calculation

The measurements results obtained in time domain will be converted in frequency domain. The impedance can be expressed as the ratio between the Fourier calculation of the voltage

and the Fourier calculation of the current which can be calculated through a FFT algorithm for all measurements. The various impedances of the equivalent circuit shown in Fig. 9 can then be determined through various configurations of the transformer.

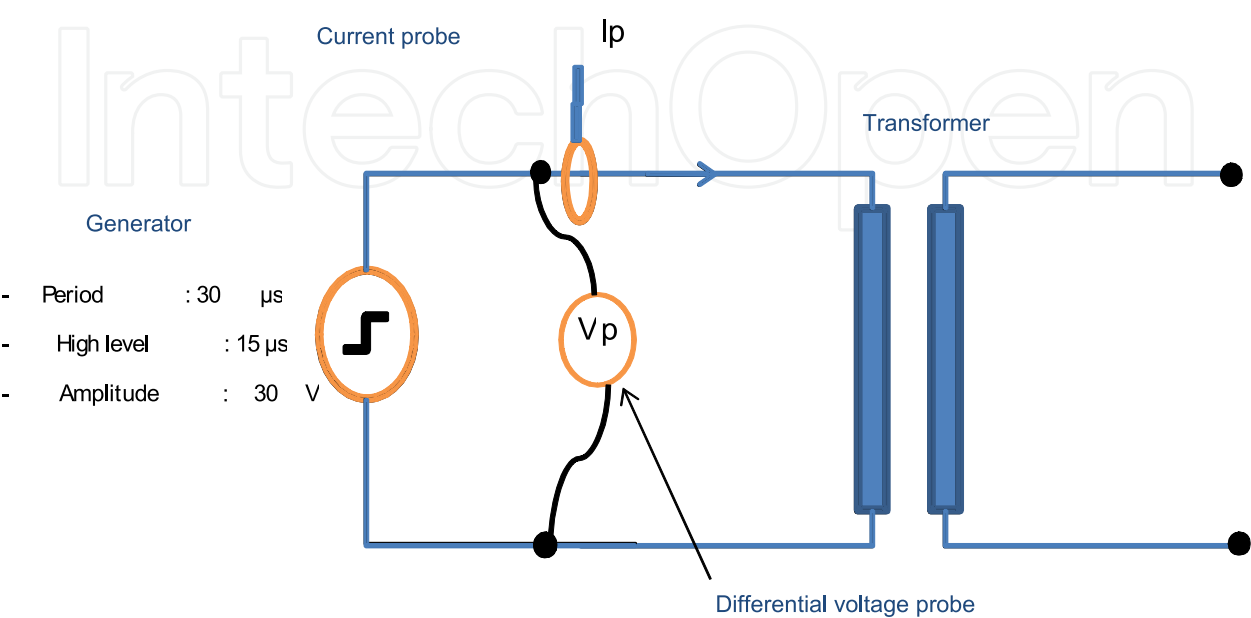


Fig. 17. Measurement bench in time domain

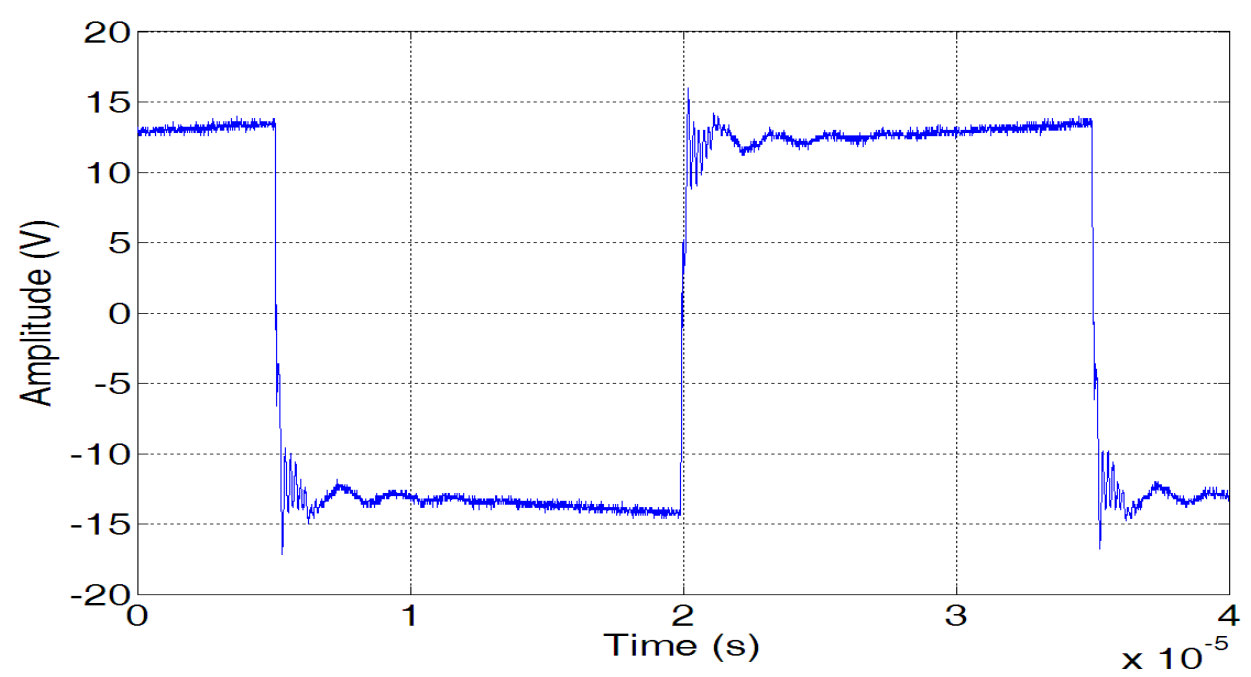


Fig. 18. Voltage waveform in primary winding when the secondary is open

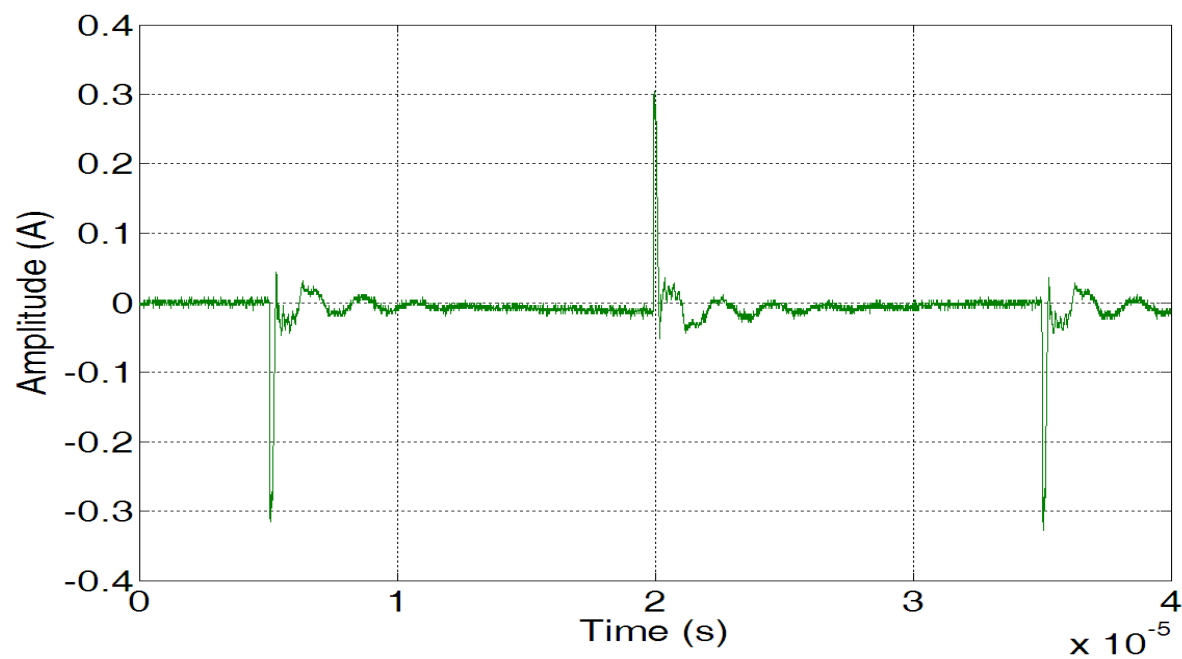


Fig. 19. Current waveform in primary winding when the secondary is open

Figure 20 shows the comparison between the impedance measured at the primary winding when the secondary is short circuited measured directly in frequency domain with impedance analyzer and the impedance issued from the data processing applied to measurements in time domain.

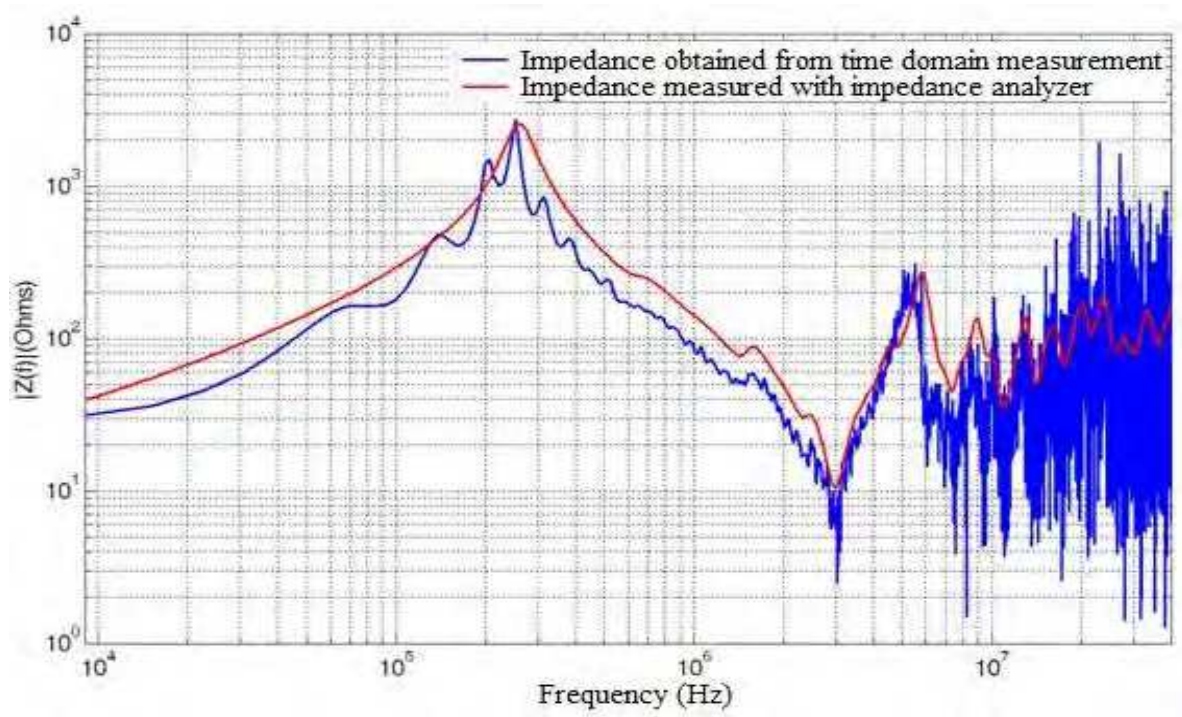


Fig. 20. Comparison between measurement of impedance in frequency domain and with temporal method applied to impedance of the primary winding, the secondary being short circuited.

The obtained results show a good agreement between these methods. However, we note a small difference, in the impedance variation between these methods in low frequency, which may be due to two reasons: the low accuracy of measurement equipments in the time domain (oscilloscope, probes ...) and the behavior of the magnetic material at low frequency.

We can say that these results validate the proposed temporal method. This method is based on measurement of the voltage and current waveforms in the study system by reference to the method of Frequency Response Analysis FRA [10] which is based on the determination of the transfer function and voltage measurements. In the proposed method, the injection of higher current values allows us to obtain the nominal operating of the transformer.

10. Application to the test bench

10.1 The laboratory setup without the line

The test bench (Fig. 8) is composed by the 15 kVA power transformer, a rectifier (twelve diodes) and a load constituted by four power resistances. The high frequency model of the power transformer is used in this simulation.

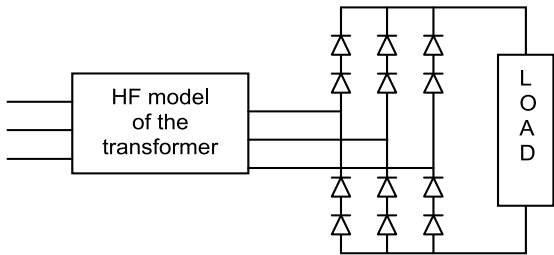


Fig. 21. Circuit diagram of the test bench

The output current of the power transformer is measured for each phase using an oscilloscope and current probe.

Figure 22 shows an example of current measured for phase A and obtained by the simulation. The test bench is simulated by using the high frequency equivalent circuit of the power transformer, presented previously, loaded with twelve diodes which model is available in the components library of the software simulator (SPICE) and four resistors.

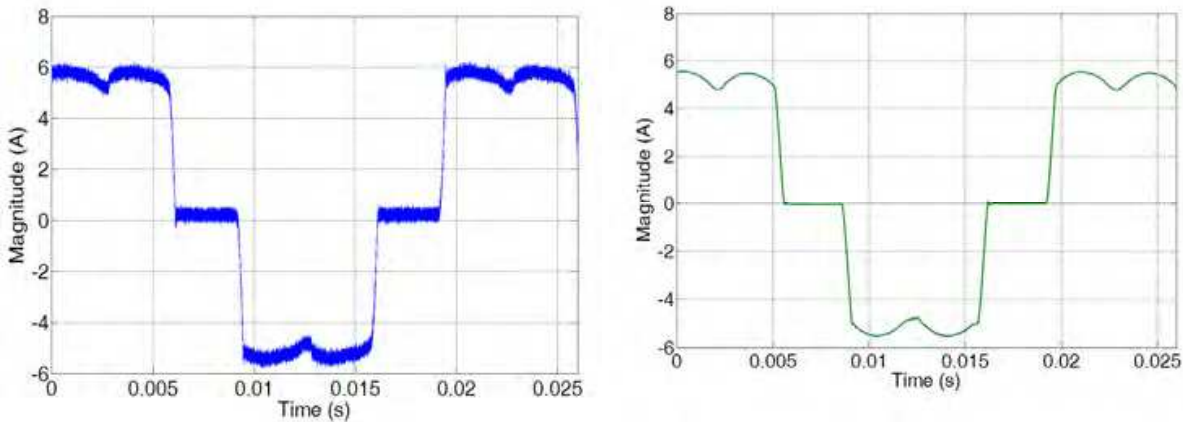


Fig. 22. Measured (left) and simulated (right) output current of the power transformer (Phase A)

As shown in Figure 22, we note a good agreement between the measured and simulated currents. Nevertheless, the waveform of the measured current is disturbed by digital noise of the oscilloscope. Moreover in our simulation we used sources without noise which does not exist in real case.

10.2 The laboratory setup with the line

As a conclusion of the laboratory study, we have realized a complete simulation of a railway power system by adding a power line and a power load to the transformer. Fig. 23 shows the experimental setup.

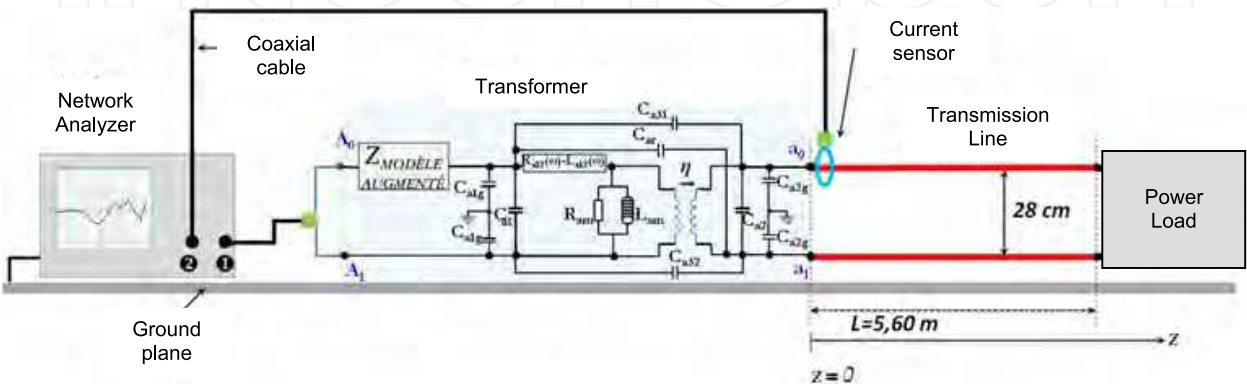


Fig. 23. Laboratory test bench simulating a railway power infrastructure

The test bench is constituted by the previous laboratory transformer (15kVA) used in one phase transformer configuration (the two others phases are short circuited), connected to a 5.6m power line and load by power resistances.

This system is fed by a network analyzer (connected to port 1) which allows measuring the current in the power line via the S_{21} parameter as presented in figure 23, thru a current sensor (connected to the port 2 of the analyzer) .

Figure 24 shows a comparison between measurements and modeling for two extreme positions of the current sensor: near the transformer ($z = 0$) and near the load ($z = 5.6$ m).

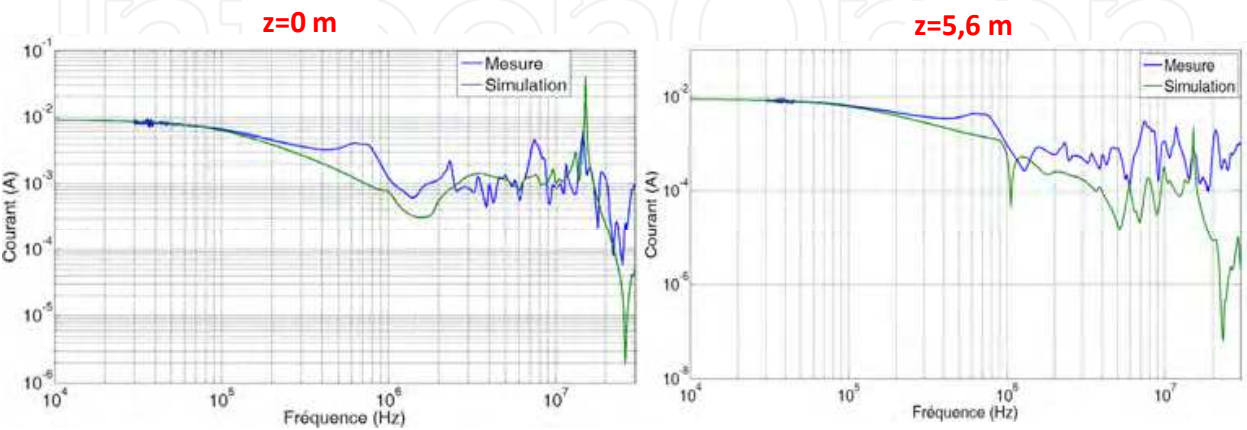


Fig. 24. Comparison between measurement and modeling : frequency variation of the current in the power line for two positions of the sensors

These curves show that the model seems very good until 10MHz. These results on a reduced scale power system are very encouraging and this study has to be continued on a real railway power substation

11. Conclusion

The results obtained with a laboratory power transformer show a good agreement between simulations and experimental results in time and in frequency domain.

Depending on the application, the measurements approach, in frequency domain, is often used and gives good results. However, for the high power system it is not possible to use an impedance analyzer (specific apparatus) thus other methods can be used as the Frequency Response Analysis (FRA). Nevertheless, the power necessary for these experimental determinations is low and can be a problem when the goal of the measurements is to define a model functioning at high power level for a large frequency band. The proposed experimental method, in time domain, allows making measurements with high injected power. The preliminary results, obtained on a laboratory transformer are very interesting.

12. Acknowledgment

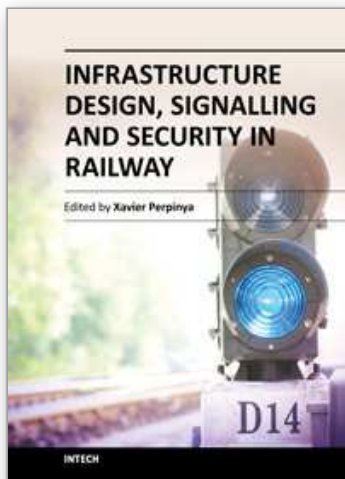
This work has been done with the help of V. Deniau and J. Rioult from IFSTTAR LEOST laboratory and G. Nottet from Alstom Transport within CEMRAIL project, with competitiveness cluster I-TRANS

13. References

- [1] European Standards EN 50121: 2006 Railway applications - Electromagnetic Compatibility.
- [2] A. Cozza, "Railways EMC : assessment of infrastructure impact" PhD thesis Lille and Torino, 2005
- [3] C. Andrieu, E. Dauphant and D. Boss, "A frequency-Dependant Model for a MV/LV Transformer", IPST'99 - International Conference on Power Systems Transient, June 20-24, 1999, Budapest
- [4] H. Ouaddi, S. Baranowski, N. Idir "High frequency modelling of power transformer : application to railway substation in scale model", XIV International Symposium on Electromagnetic Fields in Mechatronics, Electrical and Electronic Engineering, Arras, France, September 2009.
- [5] J. Kolstad, C. Blevins, J. Dunn, A. Weisshaar, "NewCircuit Augmentation Method for Modeling of Interconnects and Passive Components", IEEE Trans, Advanced packaging, Vol. 29, no.1, February 2006
- [6] www.emc.polito.it section IDEM®.
- [7] S. Chimklai, J.R. Marti, "Simplified Three-Phase Transformer Model for Electromagnetic Transient Studies", IEEE Trans, Power Delivery, vol. 10, no. 3, July 1995, pp. 1316-1325.
- [8] H. Ouaddi, S. Baranowski, N. Idir "High frequency modelling of power transformer: Application to railway substation in scale model" *Przegląd Elektrotechniczny* (Electrical Review), ISSN 0033-2097, R.86 May 2010. pp 165-169.

- [9] H. Ouaddi, S. Baranowski, G. Nottet, B. Demoulin, L. Koné, "Study of HF Behaviour of Railway Power Substation in Physical and Geometrical Scale" *European Phys. J., Appl. Phys.*, 53, 3 (2011) 33603-1-7 February , 2011
- [10] WG A2.26 report. "Mechanical condition assessment of transformer windings using frequency response analysis (FRA)" *Electra* n°228 October 2006.
- [11] H. Ouaddi, G. Nottet S. Baranowski, L. Koné, N. Idir, 'Determination of the high frequency parameters of the power transformer used in the railway substation', *IEEE VPPC 2010, Lille*, 1-3 September 2010. proceeding sur clef USB
- [12] A. Oguz Soysal, "A method for wide frequency range modelling of power transformers and rotating machines", *IEEE Transactions on Power Delivery*, vol. 8, No. 4, pp. 1802-1810, October 1993.
- [13] B. Gustavsen and A. Semlyen, "Rational approximation of frequency domain response by Vector Fitting", *IEEE Trans, Power Delivery*, vol. 14, no. 3, July 1999, pp. 1052-1061
- [14] B. Cogitore, J. P. Kéradec, "The two-winding transformer: an experimental method to obtain a wide frequency range equivalent circuit", *IEEE transactions on instrumentation and measurement*, Vol. 43, No. 2, April 1994.
- [15] T. Noda, H. Nakamoto, S. Yokoyama, "Accurate modeling of core-type distribution transformers for electromagnetic transient studies", *IEEE transactions on power delivery*, Vol.17, October 2002.
- [16] F. Blache, J. P. Kéradec, B. Cogitore, "Stray capacitance of two winding transformers: equivalent circuit, measurements, calculation and lowering", *IEEE tr IEEE transactions on Powers Electronics Specialists Conference*, 1994.
- [17] H.Y. Lu, J.G. Zhu, V.S. Ramsden, S.Y.R. Hui, "Measurement and modeling of stray capacitance in high frequency transformers", *IEEE transactions on Powers Electronics Specialists Conference*, Vol. 2, Page(s): 763 – 768, 1999.
- [18] I. A. Maio, P. Savin, I. S. Stievano, F. Canavero, " Augmented models of high frequency transformees for SMPS", *Proceeding, 20th Int. Zurich Symposium on EMC, Zurich* 2009.

IntechOpen



Infrastructure Design, Signalling and Security in Railway

Edited by Dr. Xavier Perpinya

ISBN 978-953-51-0448-3

Hard cover, 522 pages

Publisher InTech

Published online 04, April, 2012

Published in print edition April, 2012

Railway transportation has become one of the main technological advances of our society. Since the first railway used to carry coal from a mine in Shropshire (England, 1600), a lot of efforts have been made to improve this transportation concept. One of its milestones was the invention and development of the steam locomotive, but commercial rail travels became practical two hundred years later. From these first attempts, railway infrastructures, signalling and security have evolved and become more complex than those performed in its earlier stages. This book will provide readers a comprehensive technical guide, covering these topics and presenting a brief overview of selected railway systems in the world. The objective of the book is to serve as a valuable reference for students, educators, scientists, faculty members, researchers, and engineers.

How to reference

In order to correctly reference this scholarly work, feel free to copy and paste the following:

S. Baranowski, H. Ouaddi, L. Kone and N. Idir (2012). EMC Analysis of Railway Power Substation Modeling and Measurements Aspects, Infrastructure Design, Signalling and Security in Railway, Dr. Xavier Perpinya (Ed.), ISBN: 978-953-51-0448-3, InTech, Available from: <http://www.intechopen.com/books/infrastructure-design-signalling-and-security-in-railway/emc-analysis-of-railway-power-substation-modeling-and-mesurements-aspects->

INTECH
open science | open minds

InTech Europe

University Campus STeP Ri
Slavka Krautzeka 83/A
51000 Rijeka, Croatia
Phone: +385 (51) 770 447
Fax: +385 (51) 686 166
www.intechopen.com

InTech China

Unit 405, Office Block, Hotel Equatorial Shanghai
No.65, Yan An Road (West), Shanghai, 200040, China
中国上海市延安西路65号上海国际贵都大饭店办公楼405单元
Phone: +86-21-62489820
Fax: +86-21-62489821

© 2012 The Author(s). Licensee IntechOpen. This is an open access article distributed under the terms of the [Creative Commons Attribution 3.0 License](https://creativecommons.org/licenses/by/3.0/), which permits unrestricted use, distribution, and reproduction in any medium, provided the original work is properly cited.

IntechOpen

IntechOpen